Structural Engineering and Mechanics, *Vol. 71, No. 3 (2019) 233-244*
DOI: https://doi.org/10.12989/sem.2019.71.3.233

An interface model for the analysis of the compressive behaviour of RC columns strengthened by steel jackets

Giovanni Minafò*

University of Palermo, Department of Engineering, Viale delle Scienze Ed.8, 90128 Palermo, Italy

(Received September 30, 2018, Revised April 1, 2019, Accepted April 1, 2019)

Abstract. Steel jacketing technique is a retrofitting method often employed for static and seismic strengthening of existing reinforced concrete columns. When no continuity is given to angle chords as they cross the floor, the jacket is considered "indirectly loaded", which means that the load acting on the column is transferred partially to the external jacket through interface shear stresses. The evaluation of load transfer mechanism between core and jacket is not straightforward to be modeled, due to the absence of knowledge of a proper constitutive law of the concrete-to-steel interface and to the difficulties in taking into account the mechanical nonlinearities of materials. This paper presents an incremental analytical/numerical approach for evaluating the compressive response of RC columns strengthened with indirectly loaded jackets. The approach allows calculating shear stresses at the interface between core and jacket and predicting the axial capacity of retrofitted columns. A proper constitutive law is proposed for modelling the interaction between the steel and the concrete. Based on plasticity rules and the non-linear behaviour of materials, the column is divided into portions. After a detailed parametric analysis, comparisons are finally made by theoretical predictions and experimental results available in the literature, showing a good agreement.

Keywords: steel jacketing; no-end connections; retrofit; interface

1. Introduction

The use of concrete or steel jackets around RC columns is a widespread technique for static and seismic retrofitting applications (Yuce *et al*. 2007, Di Ludovico *et al*. 2008). Several literature studies proved that the structural performances of beams (Ahmedt *et al*. 2000, Oehlers *et al*. 2000) and columns can be enhanced in terms of achievable load carrying capacity, deformation capacity and stiffness. Steel jackets can be applied to existing RC columns by two possible configurations (Thermou and Elnashai 2006), depending on the connection given to the angle chords as they cross the floors. If end-connections are provided, the jacket is considered directly loaded and the axial load is transferred to the whole section, the latter acting as a whole steel-concrete composite element (Fig. 1a). In this way, the complete increase of axial capacity can be exploited and the contribution of the steel angles to the strength is directly related to their effective area. Consequently, the application of directly loaded angles should be the most convenient method for a retrofit intervention due to its theoretical maximum effectiveness. Despite this advantage, detailing of connections is a difficult task due to the introduction of plates and bars, which should be well anchored to the slabs.

For this reason, the most of technical codes allows the installation of the jacket only by indirect loading.

In this last case, steel angles have no-end connections, and a gap of few centimetres is left between the jacket and the top and bottom extremities of the column (Fig 1b).

(a) (b)

Fig. 1 Steel jacketed columns. a) Directly loaded jacket; b) Indirectly loaded jacket. (Redrawn from Campione *et al*. 2017)

The axial load acting on the column is then transferred to the jacket through shear stresses along the interface between the concrete surface of the column and the steel angles. This load sustained by the external jacket is not simple to be calculated, due to the involvement of several parameters, such as the geometry, the non-linear constitutive laws of materials and load conditions of the column. Technical standards indicate to assess the efficiency of the technique only by considering confinement effects induced by the external jacket to the inner column (CEN 2005a), and usually the contribution of jacket is neglected (CEN 2005b) in the case of indirectly loading.

*Corresponding author, Ph.D. Assistant Professor
E-mail: giovanni.minafo@unipa.it

ISSN: 1225-4568 (Print), 1598-6217 (Online)

Several works were developed in the literature to study the efficiency of steel jacketing in enhancing the structural performances of weak columns, and most of these studies investigated the case of jackets with pinned ends (Montuori and Piluso 2009; Nagaprasad *et al*. 2009; Tarabia and Albakry 2014), while few studies focused on the load transfer at the core-to-jacket interface in indirectly loaded members. Among these last, the most of studies in the literature focused only on members with reinforced concrete jacketing (Vandoros and Dritsos 2006, Achillopoulou 2017).

Adam *et al*. (2009) presented a parametric study performed by non-linear finite element (FE) simulations, the latter carried out with the aim of analysing the behaviour of RC columns strengthened by steel caging. Researchers modelled force transmission at steel-to-concrete interface via contact elements with Coulomb's friction and validated their models with experimental data of Gimenez *et al*. (2009).

Badalamenti *et al*. (2010) proposed an analytical model able to take into account the variation of confinement pressure as a function of the axial shortening. In this model, relative slip of the steel jacket is taken into account by limiting the confinement pressure to a maximum value, which depends by the friction coefficient. Belal *et al*. (2015) tested seven RC columns with different steel jacket's configurations. Specimens were retrofitted with angles, channels or plates and they were indirectly loaded. Researchers found increases of the axial strength up to 20%, but their FE simulations overestimated the load-carrying capacity of jacketed specimens up to 58% of the experimentally recorded data.

A recent experimental study on the compressive behaviour of RC columns with indirectly loaded jackets was performed by Campione *et al*. (2017). Two series of RC columns with different concrete grade and retrofitted by steel jackets with no-end connections applied by mortar were tested under axial or eccentrical compression. Tests have shown that the behaviour of retrofitted columns in terms of axial load vs. shortening curve was intermediate between the analytical prediction under the assumptions of only confinement and that of overall contribution of the external jacket.

Based on obtained results, Campione *et al*. (2017) proposed a fictitious constitutive law of the angles in compression. It was a bilinear elastoplastic law, in which peak stress was calculated by considering the maximum load transferred at interface under the assumption of Mohr-Coulomb friction criterion, while the strain corresponding to peak stress was set arbitrarily equal to strain corresponding to peak stress of concrete in compression. Despite this approach allows easy calculations, it is clear that it is based on empirical assumptions, and it is not able to predict the stress state along the interface, but only the macroscopic behaviour in terms of load capacity.

Literature review highlights that mechanically-based analytical models are still missing in this field, and no analytical model is available to study load transmission mechanisms in steel jacketed members. Previous studies proposed some models based on simplified or empirical assumptions, or on FE simulations, which require the calibration of several parameters and a great computational effort. In this work, the problem is investigated through an analytical model, which idealized the interaction of three plane elements connected by a non-linear interface. Closed form solution of the model is given under the assumption of elastic behaviour of constituent materials, allowing to make some considerations for low levels of axial shortening. Aiming to extend the model to materials with non-linear behaviour, a more reliable constitutive law of the steel-to-concrete interface is proposed, based on a plasticity approach, simplified in a bilinear law for practical implementation. Finally, an algorithm is proposed for RC members, accounting for the non-linear behaviour of concrete, by a piece-wise subdivision of the member in small portions, and considering a proper constitutive law of the concrete core and steel jacket in compression and interface. Results achieved by proposed model are then compared with experimental data available in the literature, showing good agreement. The proposed approach could be an alternative tool to more complex FE simulations for calculating the complete response of RC members strengthened by steel jackets.

2. Elastic analysis

The case study refers to a model of column subjected to an imposed axial shortening δ, with an indirectly loaded jacket placed adjacently at the sides (Fig. 2). Preliminary assumptions are made for the geometry. In particular, a plane model with two axes of symmetry is considered, in which the half-length of the column is denoted as "l". The column -layer c- is assumed to be made with a different material from the jacket (layer j), and the two layers are connected to each other with an interface, whose properties are defined in the following.

In this section, materials are assumed to behave linearly in compression with an indefinite strength limit, while modulus of elasticity are labelled as E_c and E_j for core and jacket respectively. Force is transferred between the two layers by means of an interface, the latter assumed to transfer only shear stresses τ on the basis of relative slip s between core and jacket. The constitutive law of the interface defines a relationship between τ and s, and it is here assumed as linear elastic with stiffness equal to k_{tt}. It should be considered that this assumption can be not always reliable. In fact, usually a "stick" phase in which no slips occur is likely to occur at low stress levels. However, the solution of the problem under the hypotheses of linear elastic interface can be useful for extending the solution to more complex constitutive laws. A more detailed discussion on interface properties is made on the next section with a proposal of possible constitutive law.

The equilibrium equation along x-axis of layer j can be written as

$$\frac{dN_j(x)}{dx} = p_x(x) \tag{1}$$

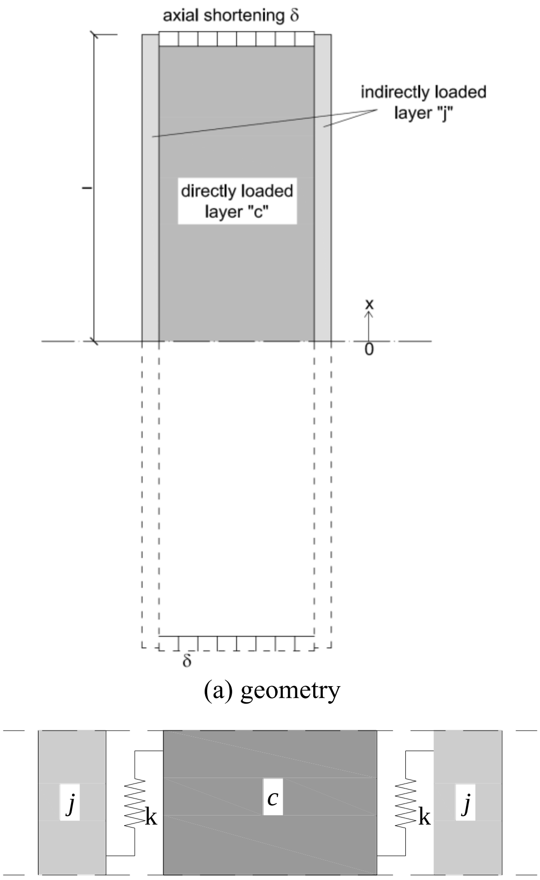

(a) geometry

(b) interface scheme

Fig. 2 Proposed model

where $p_x(x)$ is the distribution of shear forces transferred through the interface and N_j is the axial force in the layer "j". As it is well-known, internal congruence relates the normal strain ε to the axial shortening u_j, and considering the hypothesis of linear elasticity, it can be written as it follows

$$\varepsilon_j(x) = \frac{du_j(x)}{dx} = \frac{N_j(x)}{E_j \cdot A_j} \tag{2}$$

where A_j is the transverse area of the jacket.

The first order derivative of Eq.(2) can be introduced in Eq.(1), and the following relationship holds

$$\frac{d^2u_j(x)}{dx^2} = \frac{p_x(x)}{E_j \cdot A_j} \tag{3}$$

where E_j and A_j are assumed constant along the column.

Generally, the constitutive law of the interface allows relating the shear forces as a function of relative displacement between the two layers. If $u_c(x)$ is the displacement of the core, generally the shear force at the interface can be written as

$$p_x(x) = f\left(u_c(x) - u_j(x)\right) \tag{4}$$

In particular, the constitutive law of a linear pure brittle interface is written as

$$p_x(x) = k_{tt} \cdot \left(u_c(x) - u_j(x)\right) \cdot t_i \tag{5}$$

where t_i is the depth of the interface.

Therefore, if Eq.(5) is introduced in Eq.(3) the first governing equation of the problem is obtained

$$\frac{d^2u_j(x)}{dx^2} = -\frac{k_{tt}}{E_j \cdot A_j} \cdot \left(u_c(x) - u_j(x)\right) \cdot t_i \tag{6}$$

Similarly, the equilibrium of the "c" layer can be expressed as

$$\frac{dN_c(x)}{dx} = -2 \cdot p_x(x) \tag{7}$$

doing the substitutions similar to that written for layer "j", the second governing equation can be written

$$\frac{d^2u_c(x)}{dx^2} = \frac{2 \cdot k_{tt}}{E_j \cdot A_j} \cdot \left(u_c(x) - u_j(x)\right) \cdot t_i \tag{8}$$

Eqns.(6) and (8) express a coupled system of two second order differential equations, ruling the force transmission in a system of three elastic beams connected by a linear interface. Two further parameters are now introduced conveniently

$$\beta_j = \sqrt{\frac{k_{tt} \cdot t_i}{E_j \cdot A_j}} \tag{9a}$$

$$\beta_c = \sqrt{\frac{k_{tt} \cdot t_i}{E_c \cdot A_c}} \tag{9b}$$

β_j and β_c are the relative stiffness parameters between interface and jacket or core respectively. Considering the positions of Eq.(9), the system of the two governing equations is now re-written as

$$\begin{cases} \dfrac{d^2u_j(x)}{dx^2} + \beta_j^2 \cdot (u_c(x) - u_j(x)) = 0 & (10a) \\ \dfrac{d^2u_c(x)}{dx^2} - 2\beta_c^2 \cdot (u_c(x) - u_j(x)) = 0 & (10b) \end{cases}$$

The solution of the system can be obtained more easily if the system is usefully uncoupled, aiming to find a unique governing equation. The field of displacement in the core $u_c(x)$ can be explicited by Eq.(10 a)

$$u_c(x) = u_j(x) - \frac{1}{\beta_j^2} \frac{d^2u_j(x)}{dx^2} \tag{11}$$

and the second order derivative of Eq.(11) holds

$$\frac{d^2u_c(x)}{dx^2} = \frac{d^2u_j(x)}{dx^2} - \frac{1}{\beta_j^2} \frac{d^4u_j(x)}{dx^4} \tag{12}$$

Eq.(12) can be introduced in Eq.(10 b), and the short form of the governing equation is finally obtained by multiplying both sides for β_j^2.

$$\frac{d^4u_j(x)}{dx^4} - \beta_j^2 \cdot \frac{d^2u_j(x)}{dx^2}\left(1+2\frac{\beta_c^2}{\beta_j^2}\right) = 0 \tag{13}$$

Eq.(13) represents the uncoupled system, which allows finding the field of displacements in the jacket and consequently that in the core by means of Eq.(12). Involved parameters are represented by the relative stiffness parameter interface-to-jacket and interface-to-core. It can be observed that when the interface is infinitely deformable (i.e. $\beta_j=\beta_c=0$), Eq. (13) is the differential equation of axial elastic line in an axially loaded beam element.

The solution of this homogeneous fourth-order differential equation is written in the form

$$u_j(x) = c_1 \cdot \frac{e^{x\sqrt{2\beta_c^2+\beta_j^2}}}{2\beta_c^2+\beta_j^2} + c_2 \cdot \frac{e^{-x\sqrt{2\beta_c^2+\beta_j^2}}}{2\beta_c^2+\beta_j^2} + c_3 \cdot x + c_4 \tag{14}$$

where c_1,c_2,c_3 and c_4 are the unknown constants to be calculated by enforcing the boundary conditions. These last can be written as it follows

$$u_j(0)=0 \tag{15a}$$

$$u_c(0) = \left.\frac{d^2u_j(x)}{dx^2}\right|_{x=0} = 0 \tag{15b}$$

$$u_c(l) = -\frac{1}{\beta_j^2}\left.\frac{d^2u_j(x)}{dx^2}\right|_{x=l} = \delta \tag{15c}$$

$$N_j(l) = \left.\frac{du_j(x)}{dx}\right|_{x=l} = 0 \tag{15d}$$

where Eqs.(15a,b) are the symmetry conditions in x=0, Eq.(15c) is the compatibility condition at the top section of the core (x=l) and Eq.(15d) represents the equilibrium of the jacket for x=l.

Eqs.(15) is the set of equations which allows finding the constants appearing in Eq.(14) and solving the elastic problem. After constants are known, the expression of $u_j(x)$ is found and it is expressed as

$$u_j(x) = \frac{\delta \cdot \beta_j^2\left(x\cdot\eta\cdot\mathrm{Cosh}(\eta l) - \mathrm{Sinh}(\eta x)\right)}{\beta_j^2\cdot\eta l\cdot\mathrm{Cosh}(\eta l) + 2\beta_c^2\cdot\mathrm{Sinh}(\eta l)} \tag{16}$$

where $\eta=\sqrt{2\beta_c^2+\beta_j^2}$, while the field of displacements in the core $u_c(x)$ is evaluated by means of Eq.(11) and second order derivative of Eq.(16), leading to the following function

$$u_c(x) = \frac{\delta\cdot\left(x\cdot\beta_j^2\cdot\eta\cdot\mathrm{Cosh}(\eta l) + 2\beta_c^2\cdot\mathrm{Sinh}(\eta x)\right)}{\beta_j^2\cdot\eta l\cdot\mathrm{Cosh}(\eta l) + 2\beta_c^2\cdot\mathrm{Sinh}(\eta l)} \tag{17}$$

Axial forces in each layer are therefore evaluated by the first order derivative of Eqs.(16) and (17)

$$N_j(x) = E_jA_j\,\frac{\delta}{l}\,\frac{\beta_j^2\eta\cdot\left(\mathrm{Cosh}(\eta l) - \mathrm{Cosh}(\eta x)\right)}{\beta_j^2\eta\cdot\mathrm{Cosh}(\eta l) + 2\beta_c^2\cdot\mathrm{Sinh}(\eta l)} \tag{18}$$

$$N_c(x) = E_cA_c\,\frac{\delta}{l}\,\frac{\eta\cdot\left(\beta_j^2\cdot\mathrm{Cosh}(\eta l) + 2\beta_c^2\cdot\mathrm{Cosh}(\eta x)\right)}{\beta_j^2\eta\cdot\mathrm{Cosh}(\eta l) + 2\beta_c^2\cdot\mathrm{Sinh}(\eta l)} \tag{19}$$

It is noted that this approach is similar to the elastic method for predicting the load-displacement behaviour of a single pile (Goel and Patra 2007). The boundary conditions are different and the friction law on the boundary between the pile and the soil more complicated.

Fig. 3 shows an example of application of the elastic solution, assuming β_j=0.00123 and β_c=0.00140, and a normalised imposed shortening equal to δ/l=0.001%. Values of relative stiffness parameters were set assuming a possible example of a square column with side equal to 250 mm, strengthened with four steel angles with side equal to 60 mm and thickness of 8 mm and interface stiffness equal to 30 N/mm^3. Fig. 3a shows the trend of the axial force in both layers as along the normalised abscissa x/l of the column. It can be noted that the application of the external layer modifies the trend of the axial force, being the latter not constant along the member. Axial force in the core $N_c(x)$ reaches its maximum value at the extremities, while that in the jacket $N_j(x)$ increases up to the middle section of the member. This fact is due to the absence of slip in correspondence of the axis of symmetry x=0, which means that the two elements are perfectly connected in the middle section. The increase of relative slip at the interface $s(x)=u_c(x)-u_j(x)$ (Fig. 3b) tends to reduce the axial load in the external jacket up to the bottom and top sections, in which the external layer is totally unloaded and the force is sustained only by the core.

The trend of functions plotted in Fig. 3 are coherent with the symmetry conditions of the model, being axial forces symmetric and slippage anti-symmetric. The trend of shear stresses (Fig. 3c) can be considered almost linear in the central zone of the member (i.e. -0.5<x/l<0.5), while an intensification in the range 0.5<x/l<1 - or -1<x/l<-0.5 for symmetry- is observed. This fact highlights that the most stressed parts of interface are those located at about one-fourth of the total length from the extremities of the column, and these zones are those more subjected to possible detachment during the loading process.

3. Application to RC members: assumptions and constitutive relationships

In this section, an algorithm is presented for extending the above presented elastic analysis to RC columns. Aiming to this target, some preliminary assumptions are here made: the lateral expansion of the core is neglected; bending effects on the external jacket are assumed to be negligible; buckling of external angles is neglected. Additionally, the element is considered monotonically loaded which means that the existing stress state of the column at the moment of jacketing is not considered and as a consequence the

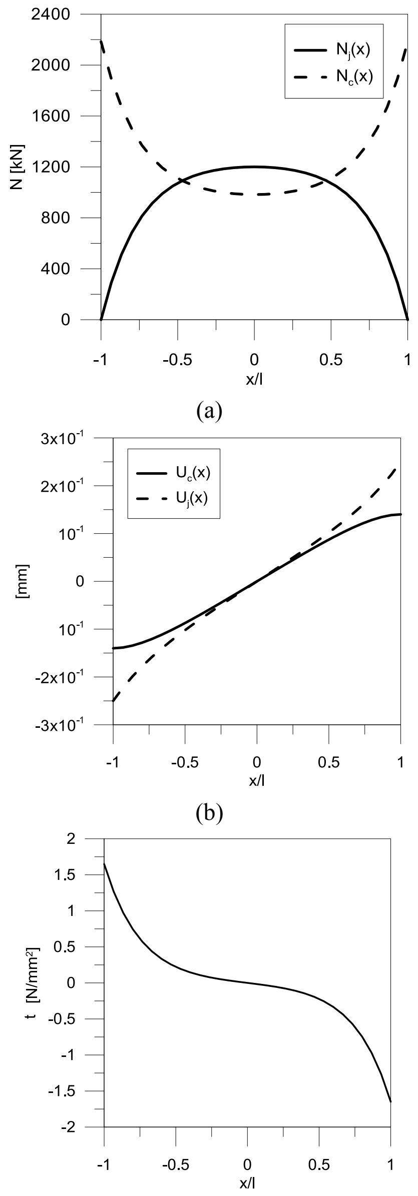

Fig. 3 Elastic solution. a) Trend of axial force; b) shortenings and relative slip at interface; c) shear forces along the interface.

proposed procedure can be applied for low values of preload. Further studies should investigate on this aspect.

Aiming to take into account the non-uniformity of concrete behaviour along the member due to the variable distribution of axial force, the previously presented model of column is divided in "n" parts with equal length "Δ" (Fig. 4) and the axial strain is assumed to be constant along each segment "i".

Transverse and longitudinal rebars inside the column are modelled through an elastic perfectly plastic law, the latter defined by means of yield stress $f_{y,i}$, elastic modulus $E_{s,i}$ and ultimate axial strain $\varepsilon_{su,i}$. Similarly, the stress-strain relation of the jacket is assumed to be elastic plastic with strain hardening. Properties of steel jacket are labelled as it follows: a yield stress $f_{y,e}$, elastic modulus $E_{s,e}$, ultimate axial strain $\varepsilon_{su,e}$ and hardening modulus E_{sh}.

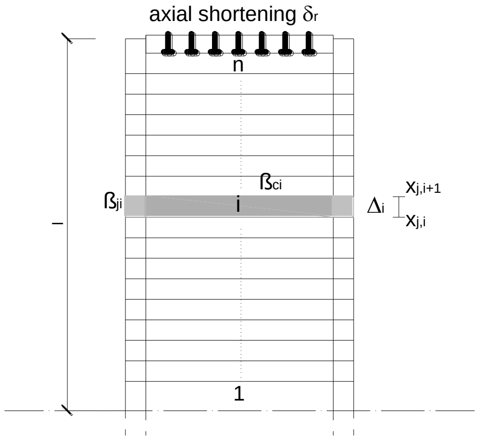

Fig. 4 Column subdivided in layers

The compressive behaviour of the RC core confined by the steel jacket and internal stirrups is modelled through the confinement model proposed by Montuori and Piluso (2009). In this model, the confinement ratios of steel battens and stirrups along the two axis of the section, ρ_z and ρ_y, are calculated in the following form:

$$\rho_z=\frac{n_z A_{s,z}\left(b\text{-}2c\right)}{s_s\left(b\text{-}2c\right)\left(h_c\text{-}2c\right)}+\frac{2A_{b,e}b}{s_b b h_c}$$
$$\rho_y=\frac{n_y A_{s,y}\left(h_c\text{-}2c\right)}{s_s\left(b\text{-}2c\right)\left(h_c\text{-}2c\right)}+\frac{2A_{b,e}h_c}{s_b b h_c} \tag{20}$$

where $A_{s,z}$ and $A_{s,y}$ are the areas of a stirrup's arms in z and y directions; n_z and n_y are the respective numbers; b and h_c are the dimensions of the cross section; s_s and s_b are the pitches of stirrups and battens; c is the concrete cover and A_b is the cross section's area of the steel battens. In general, the yield stress of steel of battens is different to that of stirrups, consequently the volumetric ratio refers to an equivalent transverse area of the battens $A_{b,e}$, defined as

$$A_{b,e}=A_b\frac{f_{y,e}}{f_{y,i}} \tag{21}$$

The lateral confinement pressures are calculated as follows:

$$f_{le,z}=k_e\cdot\rho_z\cdot f_{y,i}$$
$$f_{le,y}=k_e\cdot\rho_y\cdot f_{y,i} \tag{22}$$

being k_e the efficiency coefficient of confinement

$$k_e=\left[1\text{-}\frac{s_b\text{-}\phi_{st}}{2\left(b\text{-}2c\right)}\right]\cdot\left[1\text{-}\frac{s_b\text{-}\phi_{st}}{2\left(h_c\text{-}2c\right)}\right] \tag{23}$$

while ϕ_{st} the diameter of the stirrups. Finally, the stress-strain law of confined concrete in compression is evaluated by the expression given by Mander *et al.* (1988), which calculation is here omitted for the sake of brevity. Reference can be made to works of Montuori and Piluso (2009) for its complete definition.

4. Steel-to-concrete interface model

In the previous section, the constitutive law of the interface –i.e. the shear stress vs. slip relation- was assumed to be linear, purely brittle. It is evident that this approximation cannot be accepted for the case under consideration, in which the steel-to-concrete interaction needs to be modelled. In fact, a reliable interface law should consider the effect of normal stresses acting on its plane, i.e. the confinement pressure due to angles and battens. It is clear that a reliable interface model to be implemented in a numerical code should combine damage and friction for a cohesive zone model. However, the approach here proposed is more simplified with respect to FE simulations, and consequently a more easy law of interface is developed, reminding to literature studies (Alfano and Sacco 2006) for a more complete studies on the subject.

The basic assumption of interface models is that the thickness of the layer is so small that it can be neglected in a mathematical model. As a consequence, the layer is replaced with an interface model where displacement discontinuity can occur. In the following, the steel-to-concrete interface is studied as a zero-thickness element for which two adherents are connected through an interaction surface (i.e. a mortar layer). The following hypotheses are made: -the strain state is uniform through the contact layer; - the continuity of contact tractions occurs at the interface; - the additive decomposition in the elastic and inelastic parts is assumed for the total relative displacement.

The constitutive law of the interface relate the contact tractions to the displacement discontinuities, and the evolution of the mechanical state of the interface requires the introductions of some internal variables and the expression of relations in rate form (Cottone and Giambanco 2009). In case of detachment, the following general form of the Helmotz free energy density can be considered

$$\psi\left(\underline{U}^e,\xi\right)=\psi^e\left(\underline{U}^e\right)+\psi^i\left(\xi\right) \tag{24}$$

where Ψ^e is the elastic component of the free energy and Ψ^i is the internal one stored at the interface and related to the changes of the interface internal properties and ξ is the kinematic internal variable. $\underline{U}^e$ is the vector with components of elastic relative displacements, while the total displacement vector is written as

$$\underline{U}=\underline{U}^e+\underline{U}^p=\begin{pmatrix}u_t^e\\u_n^e\end{pmatrix}+\begin{pmatrix}u_t^p\\u_n^p\end{pmatrix} \tag{25}$$

where u_t and u_n are tangential and normal components of the relative displacement, while the superscript "e" denoted the elastic part and "p" the plastic part. Eq.(24) can be expressed in the following form

$$\psi\left(\underline{u}_e,\xi\right)=\frac{1}{2}\left(\underline{U}^e\underline{\underline{K}}\underline{U}^{eT}+h\xi^2\right) \tag{26}$$

being

$$\underline{\underline{K}}=\begin{pmatrix}k_{tt} & 0\\0 & k_{nn}\end{pmatrix} \tag{27}$$

the stiffness matrix of the interface and h the hardening/softening parameter (negative for softening behaviour).

On these bases, the rate of the free energy is written as

$$\dot{\psi}=k_{tt}u_t^e\dot{u}_t^e+k_{nn}u_n^e\dot{u}_n^e+h\xi\dot{\xi} \tag{28}$$

while the interface dissipation density assumes the following form

$$D=\underline{\sigma}^T\underline{\dot{U}}-\dot{\psi} \tag{29}$$

where $\underline{\sigma}$ is the vector of interface tractions.

$$\underline{\sigma}=\begin{pmatrix}q_t\\q_n\end{pmatrix} \tag{30}$$

The second principle of thermodynamics, taking into account the balance equation, can be written as the Clausius-Duhem inequality, which reads

$$D=\underline{\sigma}^T\underline{\dot{U}}^p-h\xi\dot{\xi}=q_t\dot{u}_t^p+q_n\dot{u}_n^p-h\xi\dot{\xi}\geq 0 \tag{31}$$

in which, Eqs.(25) and (30) were introduced.

It is worth to note that Eq.(31) is valid for every incremental deformation process, including the purely elastic ones and from the position Eq.(26) it follows that

$$\frac{\partial\psi^e}{\partial u_t^e}=k_{tt}u_t^e=q_t \tag{32a}$$

$$\frac{\partial\psi^e}{\partial u_n^e}=k_{nn}u_n^e=q_n \tag{32b}$$

The remaining partial derivative appearing in Eq.(29) allows the definition of a static internal variable energetically conjugate to ξ.

$$\frac{\partial\psi^e}{\partial\xi}=h\xi=\chi \tag{33}$$

Eqs. (32) and (33) define the interface state in both states elastic and plastic. The inelastic dissipative mechanism follows a simple linear activation function, defined in the space of static variables, which includes frictional effects

$$\phi=\left|q_t\right|+q_nTan\left(\varphi\right)-\left(a_0+\chi\right)\leq 0 \tag{34}$$

where φ is the friction angle and a_0 is the initial adhesion.

The maximum dissipation theorem i.e. maximization of the functional Eq. (31) under the admissibility conditions Eq. (34) allows to obtain the complete set of variable constitutive relations. This maximization problem can be expressed by adopting the Lagrange multiplier method, equivalent to the following unconstrained stationarity problem

$$\min_{\dot{\lambda}}\max_{\sigma,\chi}L\left(\sigma,\chi\right)=D-\dot{\lambda}\phi \tag{35}$$

where $\dot{\lambda}_p$ is the plastic multiplier. Kuhn-Tucker conditions provide the elasto-plastic laws

$$\frac{\partial L}{\partial q_t} = 0 \rightarrow \dot{u}_t^p = \dot{\lambda}_p sign(q_t) \quad (36a)$$

$$\frac{\partial L}{\partial q_n} = 0 \rightarrow \dot{u}_n^p = \dot{\lambda}_p \tan(\varphi) \quad (36b)$$

$$\frac{\partial L}{\partial \chi} = 0 \rightarrow \dot{\xi} = \dot{\lambda}_p \quad (36c)$$

with the following loading-unloading conditions

$$\phi \leq 0,\ \dot{\lambda}_p \geq 0,\ \phi\dot{\lambda}_p = 0 \quad (37)$$

Eqs. (32), (33), (36) and (37) describe the response of the interface. If the displacement history is monotonic (u>0), the following assumptions can be made

$$u^p = \xi^p = \lambda_p \quad (38)$$

The interface constitutive law reads

$$\underline{\sigma} = \underline{\underline{K}}\left(\underline{U} - \underline{U^p}\right) \quad (39)$$

Therefore, the activation function in this stage is equal to zero, and it assumes the following form

$$\begin{aligned}\phi &= k_{tt}\left(u_t - \lambda_p\right) + \\ &+ k_{nn}\left(u_n - \lambda_p\right)Tan(\varphi) - \left(a_0 + h\lambda_p\right) = 0\end{aligned} \quad (40)$$

Eq. (40) represents an equation which allows calculating λ_p. It assumes the following form:

$$\lambda_p = \frac{k_{tt}u_t + k_{nn}u_n \tan(\varphi) - a_0}{k_{tt} + k_{nn}\tan(\varphi) + h} \quad (41)$$

If Eq. (41) is introduced in Eq. (39), the following expression holds

$$q_t = k_{tt}\left(u_t - \frac{k_{tt}u_t + k_{nn}u_n \tan(\varphi) - a_0}{k_{tt} + k_{nn}\tan(\varphi) + h}\right) \quad (42)$$

It can be observed that as expected the response of the interface depends on the values of stiffness k_{tt} and k_{nn} and on internal parameters a_0 and φ. Additionally, if k_{nn} is set equal to zero, Eq.(42) provides the constitutive law proposed by Cottone and Giambanco (2009) for FRP-concrete joints in absence of normal stress. The calibration of parameters for the interface constitutive law is a difficult task, which requires experimental tests with complex set-up for considering the effect of the normal stress. In the following, some assumptions are made in order to simplify the interface model : no relative normal displacement occurs at the steel-to-concrete interface (i.e. u_n=0); the interface stiffness normally to its plane tends to infinitive – i.e. k_{nn}-->∝. Under these assumptions, the interface constitutive law Eq. (38) becomes a linear function $q_t = k_{tt}u_t$.

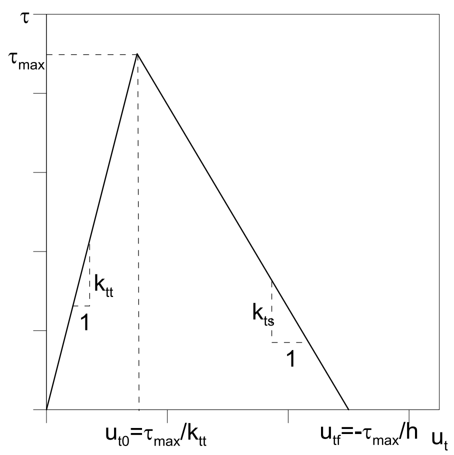

Fig. 5 Constitutive model of the interface

As a consequence in the following the assumed shear stress-slip law is that presented in Fig. 5. It is represented by the following equations:

$$\begin{cases}\tau = k_{tt}u_t \ \ for\ \ 0 \leq u_t \leq u_{t0} \\ \tau = k_{ts}(u_{tf} - u_t)\ \ for\ \ u_{t0} \leq u_t \leq u_{tf} \\ \tau = 0\ \ for\ \ u_t > u_{tf}\end{cases} \quad (43)$$

that is the simplified bilinear function suggested in Chen and Teng (2001) for steel-to-concrete interfaces. According to the approximation of a no-thick layer, the interface stiffness k_{tt} can be calculated as

$$k_{tt} = \frac{G_i}{t_i} \quad (44)$$

where G_i is the minimum shear modulus of the mortar used for placing the angles – t_i is the thickness of the interface. The maximum shear strength is calculated by the Mohr-Coulomb criterion, where the normal stress acting at the interface can be imposed equal to the confinement pressure

$$\tau_{max} = c + \mu f_{le} \quad (45)$$

where the cohesion strength c can be assumed equal to 0.1, as suggested in Adam *et al.* (2009) and the friction coefficient μ can vary in the range 0.2-0.6 as reported in Campione *et al.* (2017). Finally, f_{le} is the effective confinement pressure calculated as the minimum value between f_{lx} and f_{ly}, according to Eqs. (22).

5. Numerical procedure

Equations developed for the elastic model are introduced into an incremental procedure by following a tangent approach and solving the problem in a partitioned domain.

An axial shortening δ^r is assigned to the core and at each analysis step and a system of non-linear equations is solved through a number of iterations.

Considering the generic r-th step and its k-th iteration, the coordinates of all the portions dividing the member are resumed in the following vectors:

$$\underline{x_c^{r,k}} = \left[x_{c,1}^{r,k} \ldots x_{c,i}^{r,k} \ldots x_{c,n+1}^{r,k} \right]^T \quad (46a)$$

$$\underline{x_j^{r,k}} = \left[x_{j,1}^{r,k} \ldots x_{j,i}^{r,k} \ldots x_{j,n+1}^{r,k} \right]^T \quad (46b)$$

It is observed that for the first step (r=1), $x_{c,l}^{r,k}$ and $x_{j,l}^{r,k}$ represent the coordinates of the origin of the reference system, while the remaining components are the positions of the portions in the undeformed configuration of the column.

Stiffness parameters $E_{c,i}^{rk}$, $E_{j,i}^{rk}$ and k_{tti}^{rk} can be assigned for each part "i" to the concrete core, steel jacket and interface, on the basis of adopted constitutive laws of materials, which are known at first iteration from the elastic solution. The stiffness parameters are resumed by the coefficients β_c e β_j defined by Eqns. (9a, b), which can be written into the following vectors:

$$\underline{\beta_j^{r,k}} = \left[\beta_{j,1}^{r,k} \ldots \beta_{j,i}^{r,k} \ldots \beta_{j,n}^{r,k} \right]^T \quad (47a)$$

$$\underline{\beta_c^{r,k}} = \left[\beta_{c,1}^{r,k} \ldots \beta_{c,i}^{r,k} \ldots \beta_{c,n}^{r,k} \right]^T \quad (47b)$$

The governing equation ruling the response of the "i-th" jacket's portion is therefore written with reference to its domain

$$u_{j,i}^{r,k}(x) = c_{1,i} \cdot \frac{e^{x\sqrt{2\,\beta_{c,i}^{r,k}+\beta_{j,i}^{r,k}}}}{2\,\beta_{c,i}^{r,k}+\beta_{j,i}^{r,k}} + c_{2,i} \cdot \frac{e^{-x\sqrt{2\,\beta_{c,i}^{r,k}+\beta_{j,i}^{r,k}}}}{2\,\beta_{c,i}^{r,k}+\beta_{j,i}^{r,k}} + c_{3,i} \cdot x + c_{4,i} \quad (48)$$

$$\left\{ x_{j,i}^{r,k} \le x \le x_{j,i+1}^{r,k}, i \in [1,n] \right\}$$

being $x_{j,i}^{r,k}$ and $x_{j,i+1}^{r,k}$ are the coordinates at the extremities of the "i-th" jacket's segment.

It is noted that Eq. (48) is applied to determine the distribution of incremental relative displacement induced by imposed "shortening". Consequently, the incremental symbol should be added to $u_{j,i}^{r,k}$, but it is here omitted for the sake of clarity in the notation.

The trend of axial shortening in the core is obtained by the following relation

$$u_{c,i}^{r,k}(x) = u_{j,i}^{r,k}(x) - \frac{1}{\beta_{j,i}^{2\,r,k}} \frac{d^2 u_{j,i}^{r,k}(x)}{d^2 x} \quad (49)$$

$$\left\{ x_{c,i}^{r,k} \le x \le x_{c,i+1}^{r,k}, i \in [1,n] \right\}$$

where $x_{c,i}^{r,k}$ and $x_{c,i+1}^{r,k}$ are the coordinates at the extremities of the "i-th" core's piece. Integration constants appearing in Eq. (46) are calculated by enforcing boundary conditions for each portion. In particular, four compatibility equations can be imposed on the contact surface between the two adjacent segments

$$u_{j,i}^{r,k}(x_{j,i}^{r,k}) - u_{j,i+1}^{r,k}(x_{j,i}^{r,k}) = 0 \quad (50a)$$

$$E_{j,i}^{r,k} A_j \left. \frac{du_{j,i}^{r,k}(x)}{dx} \right|_{x=x_{j,i}^{r,k}} - E_{j,i+1}^{r,k} A_j \left. \frac{du_{j,i+1}^{r,k}(x)}{dx} \right|_{x=x_{j,i}^{r,k}} = 0 \quad (50b)$$

$$u_{c,i}^{r,k}(x_{c,i}^{r,k}) - u_{c,i+1}^{r,k}(x_{c,i+1}^{r,k}) = 0 \quad (50c)$$

$$E_{c,i}^{r,k} A_c \left. \frac{du_{c,i}^{r,k}(x)}{dx} \right|_{x=x_{c,i}^{r,k}} - E_{c,i+1}^{r,k} A_c \left. \frac{du_{c,i+1}^{r,k}(x)}{dx} \right|_{x=x_{c,i}^{r,k}} = 0 \quad (50d)$$

Constants are finally calculated by solving the previous system of Eqs. (50). The updated positions of the ends of all the column's pieces can be now calculated

$$x_{c,i}^{r,k+1} = x_{c,i}^{r,k} + u_{c,i}^{r,k}(x_{c,i}^{r,k}) \quad (51a)$$

$$x_{j,i}^{r,k+1} = x_{j,i}^{r,k} + u_{j,i}^{r,k}(x_{j,i}^{r,k}) \quad (51b)$$

The length of each piece Δ is now reduced due to the vertical displacements. It can be computed as

$$\Delta_{c,i}^{r,k+1} = x_{c,i}^{r,k+1} - x_{c,i-1}^{r,k+1} \quad (52a)$$

$$\Delta_{j,i}^{r,k+1} = x_{j,i}^{r,k+1} - x_{j,i-1}^{r,k+1} \quad (52b)$$

and the lengths obtained are subsequently resumed in the following vectors

$$\underline{\Delta_c^{r,k+1}} = \left[\Delta_{c,1}^{r,k+1} \ldots \Delta_{c,i}^{r,k+1} \ldots \Delta_{c,n}^{r,k+1} \right]^T \quad (53a)$$

$$\underline{\Delta_j^{r,k+1}} = \left[\Delta_{j,1}^{r,k+1} \ldots \Delta_{j,i}^{r,k+1} \ldots \Delta_{j,n}^{r,k+1} \right]^T \quad (53b)$$

Finally, the axial strain along each layer can be calculated as ratio between the shortening of each layer by the initial length

$$\varepsilon_{c,i}^{r,k+1} = \frac{\Delta - \Delta_{c,i}^{r,k+1}}{\Delta} \quad (54a)$$

$$\varepsilon_{j,i}^{r,k+1} = \frac{\Delta - \Delta_{j,i}^{r,k+1}}{\Delta} \quad (54b)$$

assuming that axial strain is constant along each column's piece. Once that axial strains are known by Eqs.(54), the updated values of stiffness moduli in the vectors Eqs.(47) are evaluated on the basis of adopted constitutive laws. Axial forces in all core and jacket's layers are computed from these updated values of stiffness moduli, by evaluating the first order derivative of axial shortening laws. Similarly, the shear stress at the interface of each layer is calculated by means of relative slippage between core and jacket

$$\tau_i^{r,k+1}(x) = k_i^{r,k+1} \left[u_{c,i}^{r,k+1}(x) - u_{j,i}^{r,k+1}(x) \right] \quad (55)$$

where the shear stiffness of the interface $k_i^{r,k+1}$ is updated at each step.

Afterwards, equilibrium conditions are verified at the generic k-th iteration by checking that the unbalanced residual respected a selected tolerance

$$\left[N_{c,i+1}^{r,k}\left(x_{c,i+1}^{r,k}\right)-N_{c,i}^{r,k}\left(x_{c,i}^{r,k}\right)\right]+ \\ +2\,t\,\Delta_{c,i}^{r,k}\int_{x_{c,i}^{r,k}}^{x_{c,i+1}^{r,k}}\tau_i^{r,k}(x)\,dx<tol2 \tag{56}$$

where the second addend indicates the total shear force acting along the interface of a layer, while the first term is the difference between the axial forces acting to the end of the same.

Afterwards, a successive iteration –i.e. the (k+1)-th iteration- is carried out by solving the system (48) on the basis the new values of tangent stiffness moduli and the new position of the ends of all the column's pieces (50a,b). The iterations of each load step concludes when the residual of axial strain for each layer is less than a selected tolerance

$$\left|\varepsilon_{c,i}^{r,k+1}\right|-\left|\varepsilon_{c,i}^{r,k}\right|<tol \tag{57a}$$

$$\left|\varepsilon_{j,i}^{r,k+1}\right|-\left|\varepsilon_{j,i}^{r,k}\right|<tol \tag{57b}$$

These last equations represent the convergence criteria to be applied to find the numerical solution. This task was achieved by adopting chord method and updating at each step the tangent stiffness vectors represented by Eqns.(47).

The increments of displacement δ are stopped when the ultimate axial strain of the confined concrete is achieved into a generic portion of the column.

6. Parametric analysis

A parametric analysis on obtained results is performed in order to study the influence of all parameters on the results given by the algorithm.

Constitutive laws and properties of materials are considered equal for all cases examined. In particular, all examples assume concrete compressive strength equal to 15 MPa, while the yield and ultimate stress of the steel jacket are equal to 275 MPa and 430 MPa, respectively. The constitutive law of steel is assumed to be elastoplastic with Young's modulus equal to 210000 MPa and hardening modulus 5000 MPa.

6.1 Effect of interface's stiffness

A square column with size b equal to 300 mm is considered. The overall length of the column is 2l = 820 mm, and it was divided in 12 segments. The width of the external jacket w_j is equal to 10 mm and the interface depth t is 200 mm; two values of interface stiffness k_{tt} are considered equal to 1.25 and 5.00 N/mm^3, simulating a weak interface with low grade mortar and a rigid interface with an high strength mortar. A large variation of these parameters is choose in order to check the influence of k_{tt} on the compressive response of the jacketed column.

Fig. 6 shows the trend of the axial load as a function of the axial strain, and compares the response of the retrofitted member with the two boundary cases of directly loading

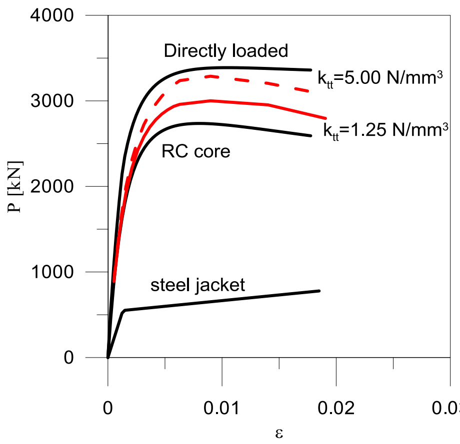

Fig. 6 Compressive behavior of steel-jacketed columns with different interface stiffness k_{tt}

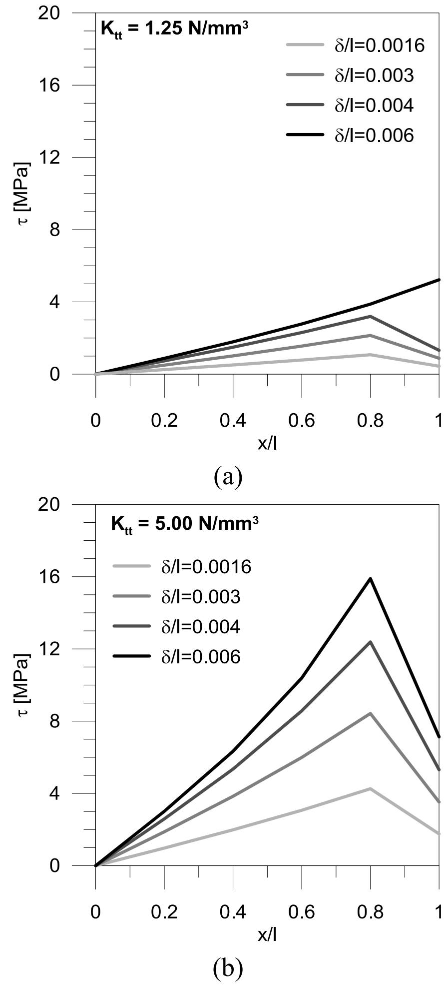

Fig. 7 Effect of interface's stiffness on the distribution of shear stresses: (a) k_{tt}=1.25 N/mm^3; (b) k_{tt}=5.00 N/mm^3

and only confinement of the RC core. The compressive response of the retrofitted column increases for increasing values of the interface stiffness, due to the greater amount of shear stress, developed at the interface and consequently due to the greater axial force sustained by the jacket. This fact is more evident from Fig. 7, which shows the trend of interface shear stress (τ) as a function of the normalized

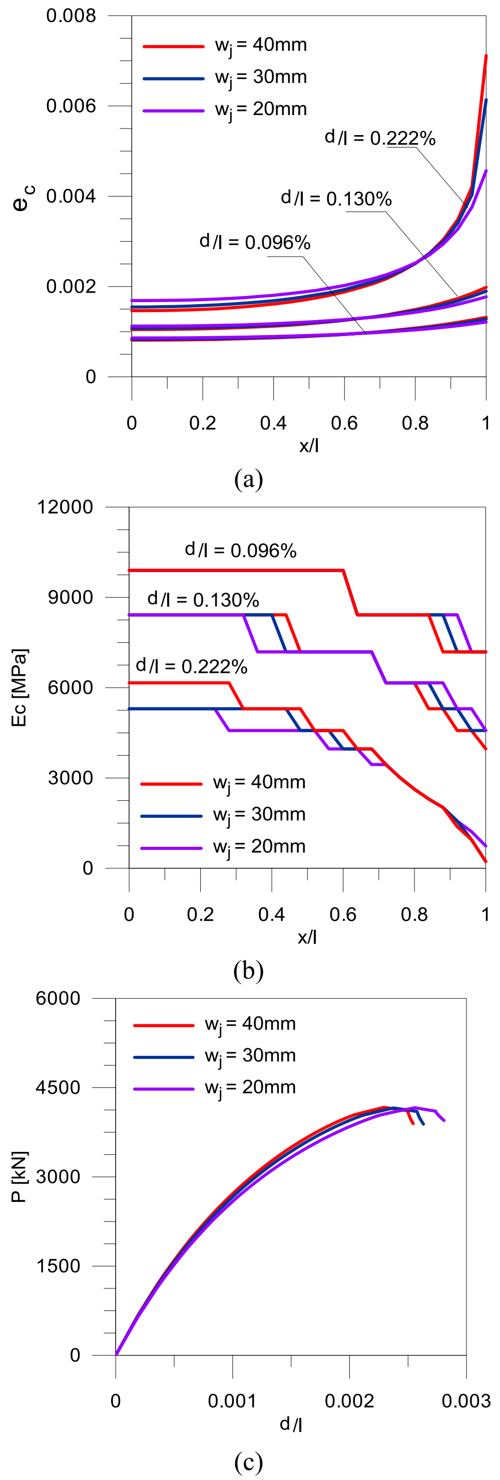

Fig. 8 Effect of jacket's width (a) axial strains along the core; (b) stiffness modulus; (c) Normalized axial shortening vs. axial load;

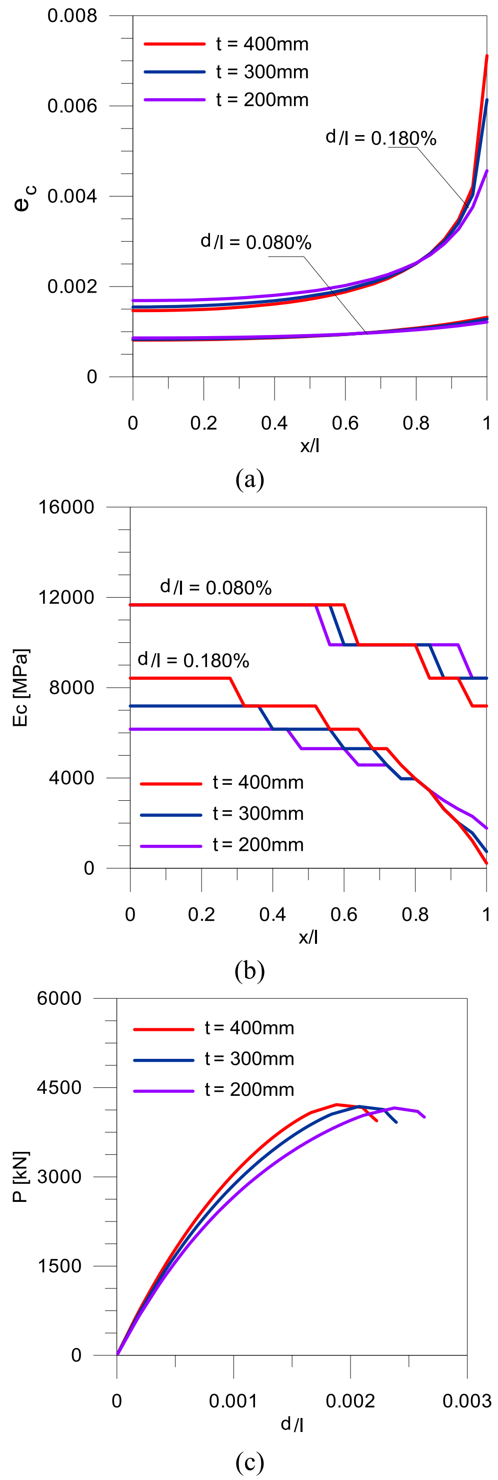

Fig. 9 Effect of interface depth: (a) axial strains along the core; (b) stiffness moduli; (c) Normalized axial shortening vs. axial load;

abscissa (x/l) and for the two values of interface's stiffness analysed. Considered functions are plotted for four analysis steps, corresponding to the imposed shortenings (δ/l) equal to 0.0016, 0.003, 0.004 and 0.006.

It is observed as similarly to the case of elastic interface, shear stresses are greater for the case of stiff interface. Shear stress increases from the centre of the member up to the maximum value, which is always achieved in correspondence of a normalized abscissa equal to x/l=0.8. It is worth to observe that interface stiffness does not affect the location of the maximum stress but only its value. After the maximum stress demand is achieved, the interface zone in the range 0.8<x/l<1 is subjected to detachment, meaning that the slip reaches higher values and the trend of the shear stresses follows the softening branch of the constitutive law.

6.2 Effect of jacket's width

Column examined in the second example has square cross section (b=400 mm) and height equal to 2l = 2500 mm, partitioned in 50 portions. The interface stiffness k_{tt} is 4.44 N/mm^3 and the interface depth t is 200 mm, while three different widths w_j were considered for the jacket, equal to 20, 30 and 40 mm. Fig. 8 shows the results in terms of axial strains, stiffness modulus of the core and the load-shortening curves calculated by proposed model. It can be observed that the width of the jacket has a small influence on the trend of axial strains, as shown in Fig. 8a, with the exception of the maximum value reached for x/l=1. In this last case, the increase of the jacket's width induces an amplification of the axial strain at the top of the column, and as a consequence the ultimate strain of the concrete is reached in an earlier step. This can be observed from the trend of stiffness moduli (Fig. 8b), and from the load-shortening curves (Fig. 8c), highlighting as the peak load of the retrofitted member is similar, but it is reached for slightly lower values of axial shortening for increasing values of w_j.

6.3 Effect of interface's depth

The last example refers to a column with the same geometrical features of the core of Example B. In this case, the width of steel angles is kept constant and equal to 30 mm, while three values of interface depth t, equal to 200, 300 and 400mm, are examined. Finally, in example C the width of steel angles is kept constant and equal to 30 mm, while three values of interface depth t, equal to 200, 300 and 400mm, are examined.

Fig. 9 shows the trend of axial strains, stiffness moduli and the load-shortening curves computed by the proposed approach. It is noted as the influence of the interface depth is similar to that achieved by the width. In fact, the distribution of axial strains and stiffness moduli is similar observed in Fig. 9a and b is similar to that shown in Fig.8. Greater axial strains are obtained at the top of the member for t=400 mm (Fig. 9a), especially for large values of shortening; on other hand, a deeper interface induces higher stiffness moduli at the centre (Fig. 9b), while the damage is concentrated at the top of the member. Consequently, also in this case the ultimate shortening of columns with larger core-to-jacket interface tends to be lower (Fig. 9c).

7. Experimental comparison

The proposed model is validated through comparisons with experimental data obtained by Campione *et al.* (2017). In this last study, two columns with rectangular cross section were considered with dimensions equal to 220x300 mm and total length 2l = 810mm. The external jacket was made by four 50x50x5 mm steel angles of grade S275; therefore, data assumed in the algorithm were thickness of the jacket equal to w_j=5 mm, interface depth t=200 mm, f_y=275 MPa, f_{su}=430 MPa, E_s=210000 MPa and E_{sh}=50000 MPa. The two columns were created concrete of different

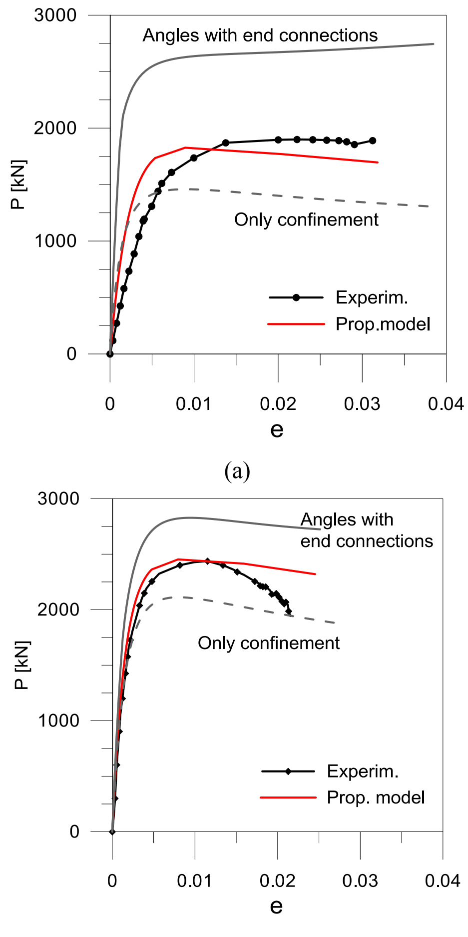

Fig. 10 Comparison between predictions of the proposed algorithm and experimental data by Campione *et al.* (2017); a) Column A; b) Column B

compressive strength. In particular, the column "A" was made with concrete grade f_c=12.65 MPa, instead, the concrete of the column "B" was grade f_c=24.00 MPa. The value adopted for the interface stiffness was k_{tt}=50 N/mm^3 for both columns. The latter are divided in 15 layers, that is each layer of the columns is high 6.66%l.

Fig. 10 shows the comparison experimental data and theoretical predictions. In particular, the axial strain vs. axial load curves of the specimens A and B obtained in Campione *et al.* (2017) are compared with the analytical predictions achieved by the proposed algorithm. Additionally, the theoretical response of the directly loaded member and that achievable only by confinement are reported. It can be observed that the proposed model is able to predict the axial capacity and the initial stiffness. The latter is overestimated in the column A due to the great initial stiffness of the constitutive law adopted for the confined core. Furthermore, the algorithm reveals a good accuracy in predicting of the post-peak branch. It is also clear that the response of the member jacketed with end connections and the response of the confined column are substantially different from the experimental result, as they represent the upper and lower bound of the compressive behaviour of the jacketed member.

8. Conclusions

This paper presented a novel analytical algorithm for predicting the compressive response of RC columns retrofitted with external jackets with no-end connections. The proposed model is based on the closed form solution valid under the assumption of linear elastic behaviour of constituent materials and of the interface. Finally, the non-linear response of RC member is taken into account partitioning the column into layers and assuming the elastic solution in each portion and introducing a possible bilinear law of the steel-to-concrete interface. From the application of the proposed approach and for the range of examined variables, the following conclusions can be drawn:

• results of parametric analysis stressed that a more rigid interface increases the axial capacity of the column. However, it is important to note that an increase of the interface stiffness leads to the intensification of the axial strain at the extremities of the column and so the overall ultimate shortening is lower;

• the increase of depth and thickness of the interface is not influent on the axial capacity of the column, but it allows to reduce shear stresses along the concrete-to-steel interface;

• the experimental validation was made by comparing analytical predictions with experimental results obtained by Campione *et al*. (2017), showing a broad good agreement. However, the comparison is limited to two results due to the lack of experimental data available in the literature. More experimental works should be addressed in the future for a correct validation of the proposed approach.

References

Achillopoulou, D.V. (2017), "Investigation of load transfer along interfaces of jacketed square columns", *Struct. Eng. Mech.,* **63**(3), 293-302. https://doi.org/10.12989/sem.2017.63.3.293.

Ahmedt, M., Oehlers, D.J. and Bradford, M.A. (2000), "Retrofitting reinforced concrete beams by bolting steel plates to their sides. Part 1. Behaviour and experiments", *Struct. Eng. Mech.,* **10**(3), 211-226. https://doi.org/10.12989/sem.2000.10.3.211

Adam, J.M., Ivorra, S., Pallarés, F.J., Giménez, E. and Calderón, P. A. (2009), "Axially loaded RC columns strengthened by steel caging. Finite element modelling", *Construct. Build. Mater.*, **23**(6), 2265-2276. https://doi.org/10.1016/j.conbuildmat.2008.11.014.

Alfano, G. and Sacco, E. (2006), "Combining interface damage and friction in a cohesive-zone model", *J. Numeric. Methods. Eng.*, **68**, 542-582. https://doi.org/10.1002/nme.1728.

Badalamenti, V., Campione, G. and Mangiavillano, M.L. (2010), "Simplified model for compressive behaviour of concrete columns strengthened with steel angles and strips", *J. Eng. Mech*., **136**(2). https://doi.10.1061/(ASCE)EM.1943-7889.0000069, 230-238.

Belal, M.F., Mohamed, H.M. and Morad, S.A. (2015), "Behavior of reinforced concrete columns strengthened by steel jacket", *HBRC J*., **11**(2),201-212. https://doi.org/10.1016/j.hbrcj.2014.05.002.

Campione, G., Cavaleri, L., Di Trapani, F. and Ferrotto, M.F. (2017), "Frictional effects in structural behavior of no-end-connected steel-jacketed RC columns: experimental results and new approaches to model numerical and analytical response", *J. Struct. Eng*., **143**(8). https://doi.org/10.1061/(ASCE)ST.1943-541X.0001796.

CEN (European Committee for Standardization) (2005a), "Design of composite steel and concrete structures. Part 1: General rules for buildings", Eurocode 4, Brussels, Belgium.

CEN (European Committee for Standardization) (2005b), "Design of structures for earthquake resistance. Part 1: General rules, seismic actions and rules for buildings", Eurocode 4, Brussels, Belgium.

Chen, J.F. and Teng, J.G. (2001), "Anchorage strength models for FRP and steel plates bonded to concrete", *J. Struct. Eng*., **127**(7), 784-791. https://doi.org/10.1061/(ASCE)0733-9445(2001)127:7(784).

Cottone, A. and Giambanco, G. (2009), "Minimum bond length and size effects in FRP–substrate bonded joints", *Eng. Fracture Mech*., **76**(13), 1957-1976. https://doi.org/10.1016/j.engfracmech.2009.05.007.

Di Ludovico, M., Balsamo, A., Prota, A. and Manfredi, G. (2008), "Comparative assessment of seismic rehabilitation techniques on a full scale 3-story RC moment frame structure", *Struct. Eng. Mech.,* **28**(6), 727-747. https://doi.org/10.12989/sem.2008.28.6.727.

Giménez, E., Adam, J.M., Ivorra, S., Moragues, J.J. and Calderón, P.A. (2009), "Full-scale testing of axially loaded RC columns strengthened by steel angles and strips", *Adv. Struct. Eng*., **12**(2), 169-181. https://doi.org/10.1260%2F136943309788251704.

Goel, S. and Patra, N.R. (2007), "Prediction of load displacement response of single piles under uplift load", *Geotech. Geol. Eng*., **25**, 57. https://doi.org/10.1007/s10706-006-0006-3.

Mander, J.B., Priestley, M.J.N. and Park, R. (1988), "Theoretical stress-strain model for confined concrete", *ASCE J. Struct. Eng*., **114**(8), 1804-1826. https://doi.org/10.1061/(ASCE)0733-9445(1988)114:8(1804).

Montuori, R. and Piluso, V. (2009), "Reinforced concrete columns strengthened with angles and battens subjected to eccentric load", *Eng. Struct*., **31**(2), 539-550. https://doi.org/10.1016/j.engstruct.2008.10.005.

Nagaprasad, P., Sahoo, D.R. and Rai, D.C. (2009), "Seismic strengthening of R.C. columns using external steel cage", *Earthq. Eng. Struct. Dyn*., **38**(14), 1563-1586. https://doi.org/10.1002/eqe.917.

Oehlers, D.J., Nguyen, N.T. and Bradford, M.A. (2000), "Retroffitting by adhesive bonding steel plates to the sides of RC beams. Part 1: Debonding of plates due to flexure", *Struct. Eng. Mech.,* **9**(5), 491-504. https://doi.org/10.12989/sem.2000.9.5.491.

Tarabia, A.M. and Albakry, H.F. (2014), "Strengthening of RC columns by steel angles and strips", *Alexandria Eng. J.*, **53**(3), 615-626. https://doi.org/10.1016/j.aej.2014.04.005.

Thermou, G.E., and Elnashai, A.S. (2006), "Seismic retrofit schemes for RC structures and local–global consequences", *Prog. Struct. Engng. Mater*., **8**(1), 1-15. https://doi.org/10.1002/pse.208.

Vandoros, K.G. and Dritsos, S.E. (2006), "Interface treatment in shotcrete jacketing of reinforced concrete columns to improve seismic performance", *Struct. Eng. Mech.,* **23**(1), 43-61. https://doi.org/10.12989/sem.2006.23.1.043.

Yuce, S.Z., Yuksel, E., Bingol, Y., Taskin, K. and Faruk Karadogan, H. (2007), "Local thin jacketing for the retrofitting of reinforced concrete columns", *Struct. Eng. Mech.,* **27**(5), 589-607. https://doi.org/10.12989/sem.2007.27.5.589.

CC